Int. J. Electron. Commun. (AEÜ) 144 (2022) 154061

Contents lists available at ScienceDirect

International Journal of Electronics and Communications

journal homepage: www.elsevier.com/locate/aeue

Regular paper

Simple wideband extended aperture antenna-inspired circular patch for V-band communication systems

Musa Hussain [a], Syeda Iffat Naqvi [b], Wahaj Abbas Awan [c,*], Wael Abd Ellatif Ali [d], Esraa Mousa Ali [e], Salahuddin Khan [f], Mohammad Alibakhshikenari [g,*]

[a] Department of Electrical Engineering, Bahria University Islamabad Campus, Islamabad 44000, Pakistan
[b] Telecommunication Engineering Department, University of Engineering Technology, Taxila 47050, Pakistan
[c] Department of Computer and Communication Engineering, Chungbuk National University, Cheongju 28644, South Korea
[d] Department of Electronics & Communications Engineering, College of Engineering and Technology, Arab Academy for Science, Technology and Maritime Transport (AASTMT), Alexandria 1029, Egypt
[e] Faculty of Aviation Sciences, Amman Arab University, Amman 11953, Jordan
[f] Electrical Engineering Department, College of Engineering, King Saud University, Riyadh 11421, Saudi Arabia
[g] Department of Signal Theory and Communications, Universidad Carlos III de Madrid, 28911 Leganés, Madrid, Spain

ARTICLE INFO

Keywords:
Compact size
Wideband
High gain antenna
V-band
Communication systems

ABSTRACT

This article presents the design and realization of compact, geometrically simple, wideband and high gain antenna for V-band communication systems. The antenna is designed by using a conventional circular patch, which is further modified by using another fractal circular patch. Furthermore, the addition of three elliptical shaped patches significantly increases the bandwidth of the antenna. Afterwards, a circular slot is etched from the radiator to improve the radiation pattern of the antenna. The proposed structure comprises of an overall substrate size of $13 \times 12 \times 0.508$ mm^3 and designed using Duroid 5880 having very low loss tangent of 0.0009. To verify the presented results, the antenna prototype is fabricated and tested. The comparison among simulated and measured results shows a strong performance. Moreover, the comparison with state of the artwork shows that the antenna offers compact size, wide bandwidth, high gain, and good radiation efficiency. Thus, it makes the proposed antenna a potential candidate for the V-band communication systems.

1. Introduction

With the advent of pervasive telecommunication systems integration in devices, the future generation of communication, including 5th and 6th generation, commonly known as 5G and 6G, are under consideration [1]. Both of these telecommunication methodologies can be exploited to cater the issues like increased number of users on a single frequency spectrum, low throughput, under optimized data rate transfer, high latency rate and others. The problems can be depreciated by using mm-wave band spectrums (30–300 GHz), where 28 GHz, 38 GHz, and 60 GHz are the potential spectrums for the said purpose [2–4]. Besides, WiGig (extended version of Wi-Fi) by the Institute of Electrical and Electronics Engineering will provide access to the V-band [5]. Moreover, Federal Communication Commission (FCC) proposed 57–64 GHz band spectrum for industrial scientific and medical (ISM) applications [6]. Thus, among all other potential band spectrums for mm-wave, 60 GHz has attained relatively more attention of scientific community.

Antennas, being the backbone of any communication system, have a significant impact on designing the overall compact system [7–10]. The greater the dimension of an antenna, the greater will be the size of communicating device. A recent trend suggests a massive amount of work being carried out to design compact communication devices for both on body and off body applications, including wearables and cellular devices [11–12]. Thus, compact size antennas become a natural demand for miniaturized communication systems. Furthermore, the performance parameters including bandwidth, gain and far-field radiation characteristics should not be compromised while designing small antennas for mm-wave applications [13–14]. However, to achieve the aforementioned performance at the V-band is a highly challenging task. Therefore, a reasonable amount of compromise exists in achieving a

* Corresponding authors.
E-mail addresses: musa.hussain@ieee.org (M. Hussain), iffat.naqvi@uettaxila.edu.pk (S. Iffat Naqvi), wahajabbasawan@ieee.org (W. Abbas Awan), wael.ali@aast.edu (W. Abd Ellatif Ali), esraa_ali@aau.edu.jo (E. Mousa Ali), khanheu@gmail.com (S. Khan), mohammad.alibakhshikenari@uc3m.es (M. Alibakhshikenari).

https://doi.org/10.1016/j.aeue.2021.154061
Received 6 October 2021; Accepted 29 November 2021
Available online 4 December 2021

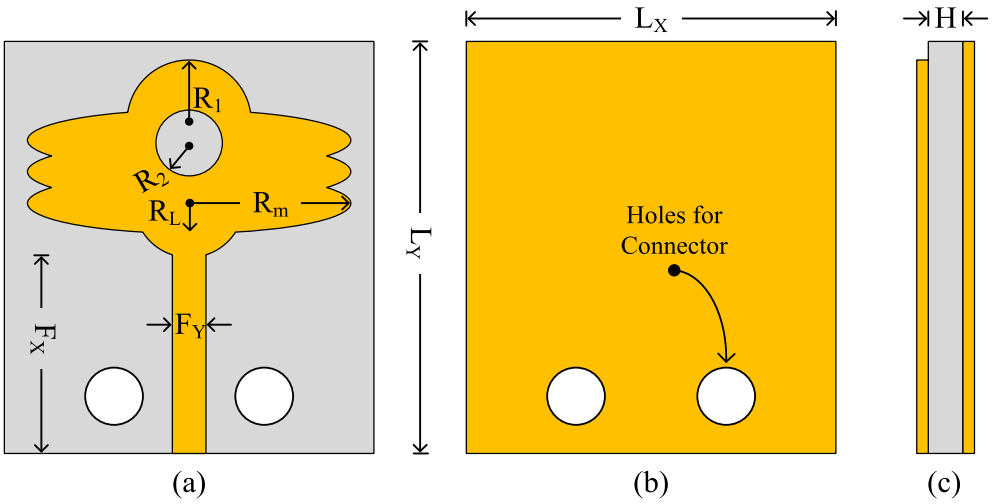

Fig. 1. The geometry of proposed antenna (a) Front View (b) Back View (c) Side view.

design of low complexity and high-level performance.

Recently, various studies have been reported in literature to develop an effective antenna for the V-band communication spectrum [15–26]. In [15], a compact size button antenna for wearable applications is proposed; however, the antenna performance parameters, including bandwidth and gain, are compromised to achieve an electrically small antenna. In another work [16], a Substrate Integrated Waveguide (SIW) based antenna is proposed for medical imaging applications, albeit the proposed work suffers from several drawbacks, including large size, narrow bandwidth, and low gain. Another interesting research is reported in [17], where the researcher design two different patches for 38 and 60 GHz frequency bands. The patches are electrically connected with each other using proximity coupling. Furthermore, the unit element is employed to achieve an array antenna having high gain at the cost of a larger area. Moreover, the limited bandwidth at both resonating frequencies is also not suitable for modern communication systems. Contrary to the previous works, a wideband wire bond antenna was presented in [18]. Although the antenna offers compact size and wideband, it also exhibits several drawbacks, including negative gain and high profile. Similarly, [19] presents another wideband antenna, where researchers designed log-periodic antenna using multiple layers to enhance the bandwidth and gain of the proposed antenna, which resulted in a complex geometrical structure along with high profile. In another work [20], an Ultra-Wide Band (UWB) antenna is designed using the concept of fractal structures and this antenna structure offers 20 GHz of operational bandwidth with a peak gain of 4 dB. Moreover, no practical performance of the antenna has been shown to validate the results. In [21], a four-element gap coupled antenna array is designed to achieve a high gain of 12 dB, however, the limited bandwidth and bigger size limits its application for compact size devices. Likewise, very high gain antenna arrays are proposed in [20–21], where the array antenna in [22] offers a peak gain of 28 dB. In comparison, a peak gain of 13 dB is obtained in [23], having a wide operational bandwidth at the cost of very large size. A wire grid antenna is designed and realized in [24]. The antenna offers a high gain of 12 dB, having a wide operational bandwidth of 8 GHz at the cost of bigger dimensions. In [25] a conventional slotted patch antenna is designed, where DGS technique is used to attain high gain. However, use of multiple defects in patch and ground significantly increased the complexity. Moreover, the achieved bandwidth of 6 GHz is also not sufficient for V-band applications. Also, a truncated ground plane dipole antenna for vehicular application in 5G communication is reported in [26]. The antenna has compact dimensions of 10 mm × 13 mm with high gain of 6.18 dBi. The reported design has setback of narrow band ranging from 49.91 to 52.15 GHz (2.24 GHz) along with complex geometry. Another interesting work is reported in [27], where a Helical inspired antenna is designed using a Through-Glass Silicon Via (TGSV). Although the reported work offers wide operational band along with high gain, but still, it suffers from limitations including complex geometrical configuration and high-cost fabrication process. Thus, considering the aforementioned state-of-the-art works, it is noticed that designing the antenna at mm-wave and particularly V-band spectrum having compact size, low complexity level, high gain and wide bandwidth is really a challenging task. However, there is still demand of an antenna that fulfills all the above-mentioned requirements.

Therefore, the presented work offers a compact size antenna for V-band applications. The antenna comprises of a simple geometrical configuration having a full ground plane owing ultra-wide bandwidth. Furthermore, the high gain and efficiency of the proposed antenna also enhanced its overall performance. Section 2 presents the design methodology of the proposed antenna, while results and relevant discussion is presented in section 3. The discussion is concluded in section 4 accompanied by reference.

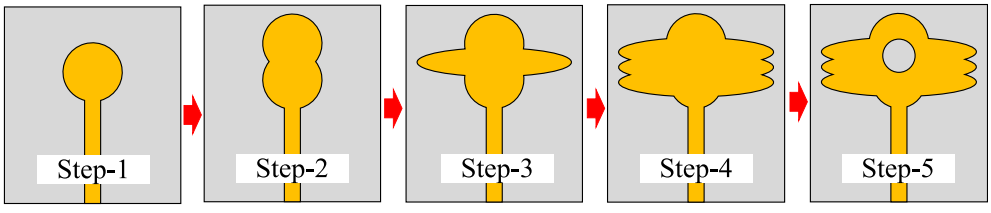

Fig. 2. Various steps to achieve the final design of the proposed antenna.

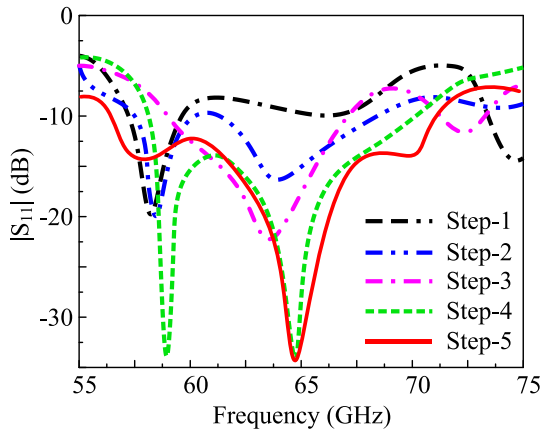

Fig. 3. Reflection coefficient comparison of the various design stage.

2. Antenna geometry and design methodology

2.1. Geometry of proposed antenna

The geometry of the proposed V-band antenna is illustrated in Fig. 1. The antenna geometry primarily consists of a circular patch antenna, where a fractal circular patch is loaded later. Afterwards, three consecutive iterations of the elliptical-shaped patch are introduced to further improve the impedance bandwidth. Lastly, a circular slot is etched from the radiator to redistribute the surface current, which results in improved bandwidth of the antenna. The antenna geometry is etched on the top side of ROGERS RT/duroid 5880, having permittivity (ε_r) and tangent loss ($tan\delta$) of 2.2 and 0.0009, respectively. The overall dimensions of the proposed antenna are $L_X \times L_Y \times H$. Two holes are also etched from the antenna for the insertion of screws of the end launch connector, used for measurement purposes. The various parameters of the antenna are optimized in each step to achieve the best possible results. The optimized parameters of the proposed wideband antenna are as follow:

$L_X = 13$ mm; $L_Y = 12$ mm; $H = 0.508$ mm; $R_1 = 1.75$ mm; $R_2 = 1.25$ mm; $R_L = 0.75$ mm; $R_M = 7$ mm; $F_X = 6.7$ mm; $F_Y = 0.5$ mm.

2.2. Design methodology of proposed Antenna:

Various steps performed to achieve the presented antenna are illustrated in Fig. 2. The antenna design process initiates with designing the conventional circular patch antenna for the central frequency. The circular patch is selected due to its advantages of single parameter responsible for generating frequency i.e., the radius of patch, along with its advantage of getting wideband as compared to other conventional structures [28]. The effective radius (R_e) of the circular patch antenna can be calculated with the help of equation (1) [28].

$$Re = R_1\left\{\sqrt{1+\frac{2H}{\pi\varepsilon r R_1}\left(\ln\frac{\pi R_1}{2H}+1.7726\right)}\right\} \tag{1}$$

here H is the thickness of the substrate, ε_r is the dielectric constant of the substrate, and R_1 is the physical radius of the circular patch which could be calculated in terms of resonate frequency using the following relation [26]

$$R_1 = \frac{F}{\left\{\sqrt{1+\frac{2h}{\pi\varepsilon r F}\left(\ln\frac{\pi F}{2H}+1.7726\right)}\right\}} \tag{2}$$

where F can be estimated using the following equation

$$F = \frac{8.79\times 109}{fr\sqrt{\varepsilon r}} \tag{3}$$

The resultant antenna exhibits the resonance across 58 GHz having $|S_{11}| < -10$ dB bandwidth of 3.6 GHz ranging from 56.8 to 60.4 GHz, as depicted in Fig. 3. In the next step, another circular patch having the same radius as of step-1 is inserted at the top side of the circular patch, as shown in Fig. 2. The center of the inserted patch is placed at the boundary of the circular antenna. This insertion results in increasing the effective length of the radiator which causes the extra flow of current along the patches. Consequently, this improves the impedance matching at 63.5 GHz and resonance is achieved at this frequency, as depicted in Fig. 3. Thus, the patch antenna at this stage exhibits dual-bands at 58.2 GHz and 63.5 GHz with respective impedance bandwidths of 3.3 GHz and 5.7 GHz.

Afterwards, an elliptical patch is loaded at the center of the patch antenna obtained in the previous step, as depicted in Fig. 2. The insertion of the elliptical patch increased the effective length of the antenna, which significantly improves the impedance matching over a wide band spectrum. The central frequency (F_C) of an elliptical patch can be estimated using the following expression (4) provided in [29]:

$$F_C = \frac{15}{\pi e R_M}\sqrt{\frac{q_c}{\varepsilon_r}} \tag{4}$$

here π is mathematical constant whose value is $\frac{22}{7}$, e is the eccentricity

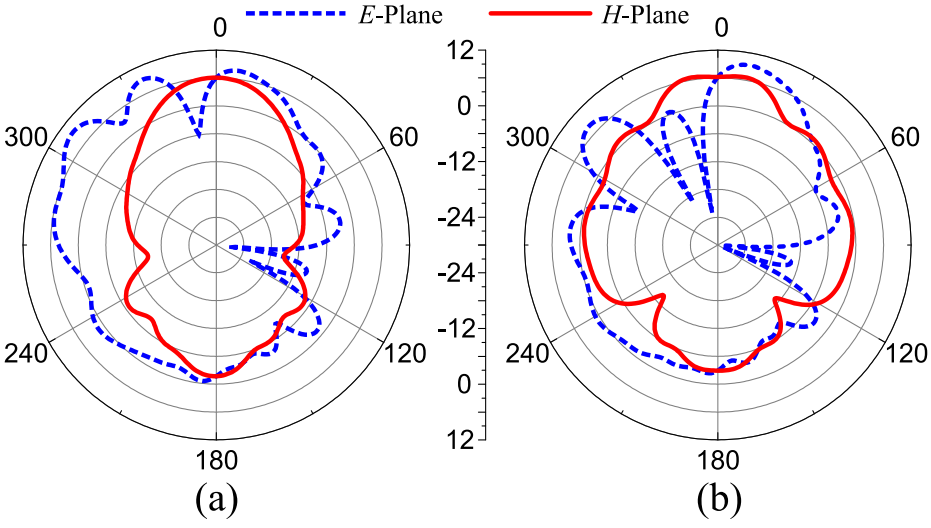

Fig. 4. The radiation pattern of the proposed antenna (a) without slot (b) with a circular slot.

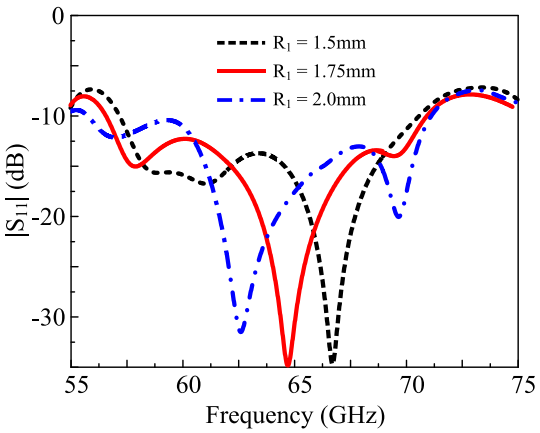

Fig. 5. Parametric analysis of patch radius (R_1).

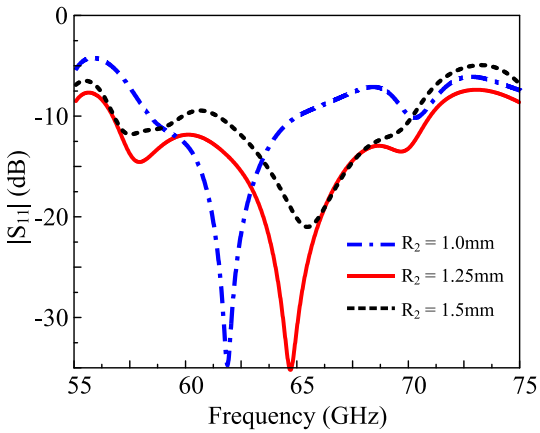

Fig. 6. Parametric analysis of slot radius (R_2).

of the ellipse, and q_c is angular Mathieu function whose value depends upon the even or odd mode of operation. A detail discussion explaining the methodology of identifying the value of angular Mathieu function can be found in [30]. The value of e can be calculated using the equation (5):

$$e = \sqrt{1 - \left(\frac{R_L}{R_M}\right)^2} \tag{5}$$

The resulted antenna offers a single wideband ranging 58.7–67.2 GHz, as depicted in Fig. 3. The next phase of the design methodology comprises loading two more elliptical patches in the radiator to achieve a wider bandwidth. It is observed that with the insertion of three elliptical patches, the bandwidth of the antenna tends to increase. However, the insertion of further elliptical patches (fourth or so on) causes a decrement in the bandwidth of the antenna. Thus, the three inserted elliptical-shaped patches are optimized to achieve maximum achievable $|S_{11}| < -10$ dB bandwidth of 58.2–70.3 GHz, as depicted in Fig. 3.

It is also observed that due to the insertion of the elliptical patches, the far-field radiation characteristics of the antenna turn out to be distorted significantly, as depicted in Fig. 4 (a). Among various techniques adopted by researchers to achieve the desirable far-filed radiations, the introduction of the slots in radiating structure is well known due to its ease of implementation. Therefore, in the last step, a circular slot is etched from the center of the radiator, as depicted in Fig. 2. Due to the annular slot the radiation pattern of the antenna shifted back towards the broadside, as depicted in Fig. 4(b). Optimization through parametric analysis is performed to achieve the best possible results. It is also observed that the circular slot further increases the bandwidth of the antenna, and the optimized antenna exhibits an ultra-wideband of 16.1 GHz (56.1–72.2 GHz), as depicted in Fig. 3.

2.3. Parametric analysis

2.3.1. Effect of radius of circular patch

The radius of the circular patch of the proposed antenna plays a vital role in controlling the shifting of the resonant frequencies. When the radius of the circular patch changes from 1.75 mm to 1.5 mm, a band shift is observed with central resonant frequency initially at 65 GHz to 67.5 GHz, as illustrated in Fig. 5. Similarly, by increasing the radius (R_1) of the patch from 1.75 mm to 2 mm, the resonating frequency shifts to 62.5 GHz, as shown in Fig. 5. However, it is observed that the overall bandwidth of the antenna remains unchanged in all cases.

2.3.2. Effect of radius of circular slot

The slot in the antenna also plays a vital role in obtaining the optimal antenna performance. Due to the incorporation of slot an improvement is observed in the bandwidth of the antenna as well as in radiation pattern, as illustrated earlier in section 2.2. The effect of the slot on the reflection coefficient is depicted in Fig. 6. When $R_2 = 1.25$ *mm*, the antenna operates at 65 GHz, having a wide impedance bandwidth of 16.1 GHz ranging (56.1–72.2 GHz). However, when the radius of slot (R_2) is changed to 1 mm or 1.5 mm, the central frequency of the antenna shifted. Also, narrowing of the bandwidth is observed with degradation in overall antenna performance. Thus, the optimized value of R_2 is set to be 1.25 mm.

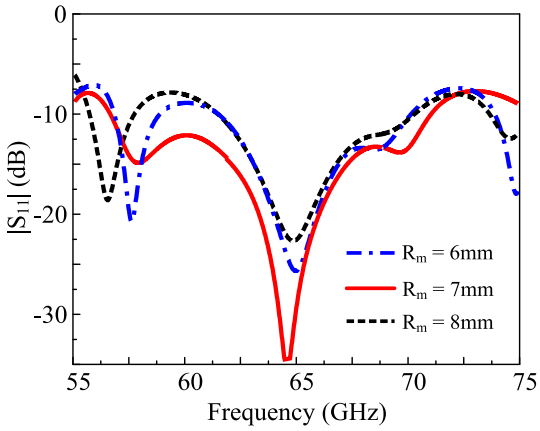

Fig. 7. Parametric analysis of major radius of ellipse (*Rm*).

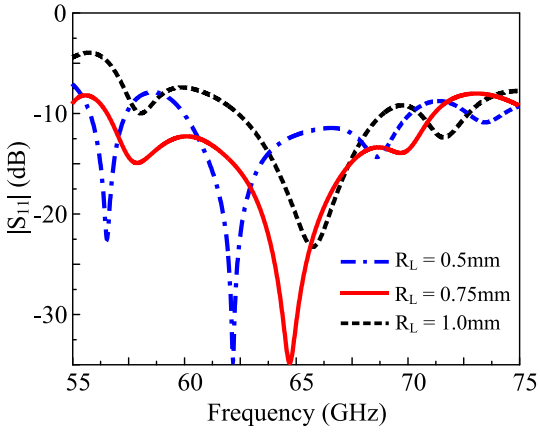

Fig. 8. Parametric analysis of minor radius of ellipse (R_L).

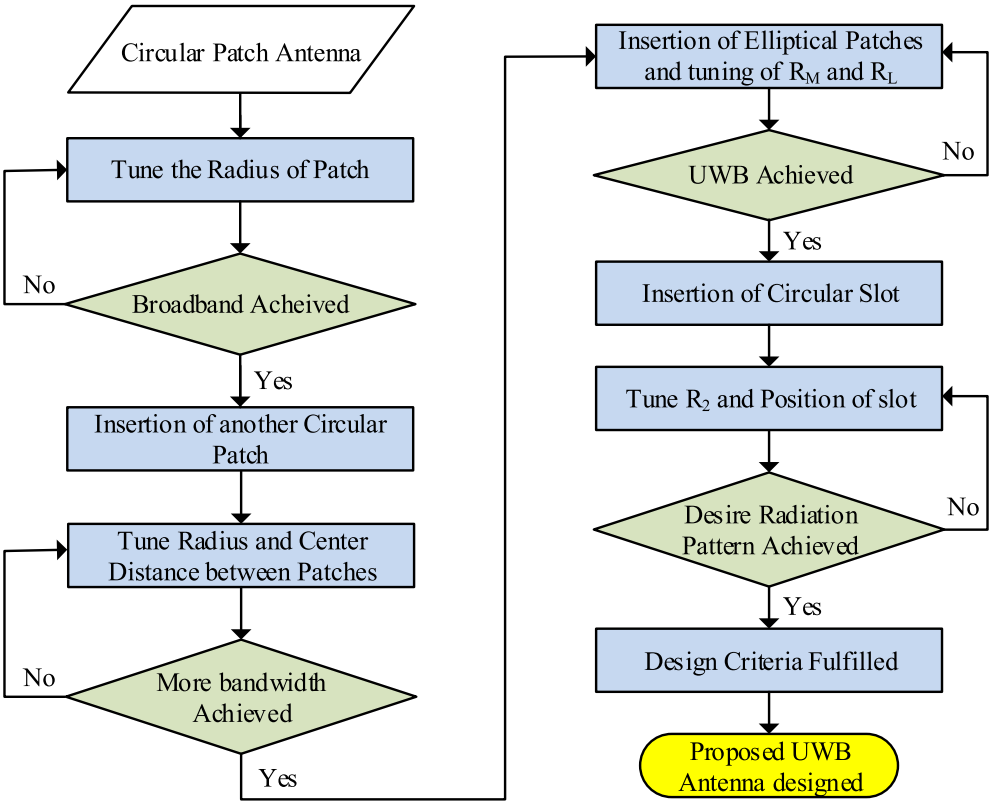

Fig. 9. Flow chart of the designing methodology adopted for proposed work.

2.3.3. Effect of ratio (length) of elliptical patch

The effects of elliptical patches are investigated in two ways, in terms of the ratio of the elliptical patches and the radius of the patches. For the proposed design, the length or ratio of elliptical patches are chosen to be $R_M = 7$ *mm*. It is observed that if the value of R_M is increased or decreased, the antenna starts resonating at dual bands, as depicted in Fig. 7. However, a notched band is obtained ranging from 57.5 to 62.5 GHz, thus narrowing the bandwidth along with band shifting towards lower frequencies. Hence, the optimized value of $R_M = 7$ *mm* offers wideband behavior and is chosen for further assessments.

2.3.4. Effect of radius of elliptical patch

Another critical parameter of the antenna that plays a vital role in controlling the resonating frequency and bandwidth of the antenna is the radius of fractal elliptical-shaped patches (R_L). When R_L is shifted from 0.75 mm to 0.5 mm, the resonating frequency shifts from 65 GHz to 62.5 GHz, as depicted in Fig. 8. Moreover, the resultant antenna with R_L = 0.5 mm offers a dual-band operational mode having a non-resonating band of 58 GHz–61.8 GHz. On the other hand, when the value of R_L is changed to 1 mm, the central frequency of the resonating band shifts from 65 GHz to 66.7 GHz, as shown in Fig. 8. Furthermore, the operational bandwidth of the antenna also reduces significantly. Thus, the

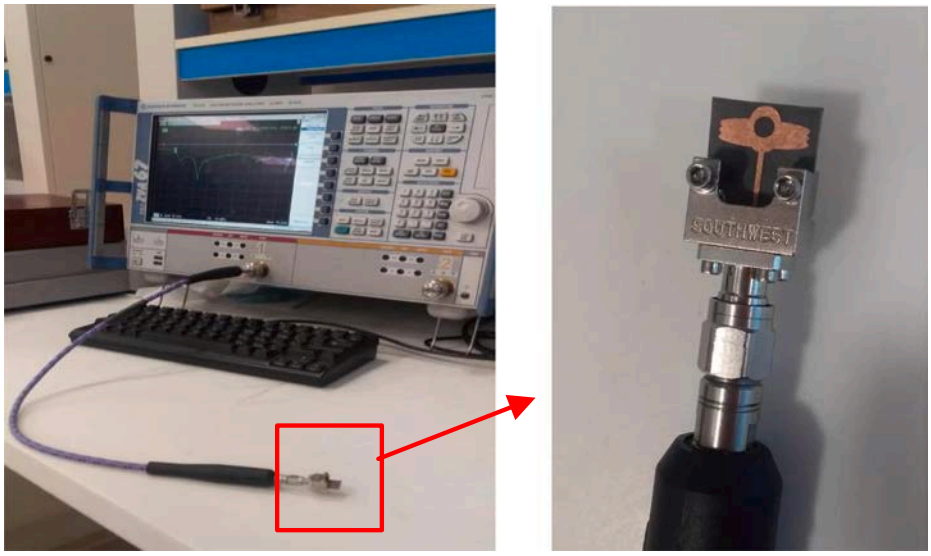

Fig. 10. Fabricated prototype along with reflection coefficient measurement setup.

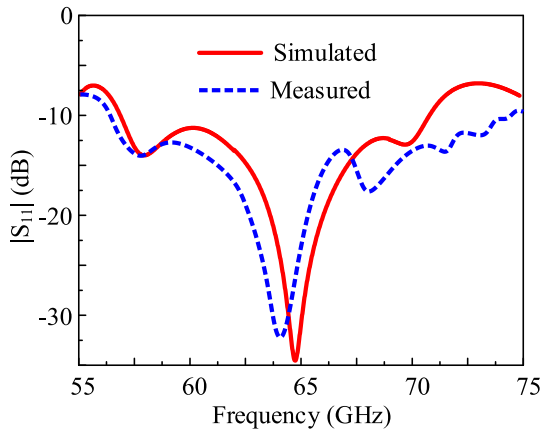

Fig. 11. Comparison among predicted and measured reflection coefficient of proposed wideband antenna.

optimal value of R_L is 0.75 mm.

2.4. Antenna design methadology

In Fig. 9, the flow chart of proposed antenna is given. Initally, the circular patch monopole antenna is designed by using equations given in section 2.2. After that the radius of the patch is tuned to obtain the wideband for trageted frequency. After that another circular patch is added to further increase the bandwidth. At this stage, the raduis of the circle as well as the central distance between patches is modified to achive more wideband. Afterwards, three elliptical stubs are introduced between two circular patches, and the major (R_L) and minor (R_M) radius of the ellpises are adjusted to obatin ultra-wideband. In the last step, a circular slot is echted from design. The radius of the circular slot (R_2) and its position is altered until the desired radition pattern is obtained. Consequently, the desired ultra-wide band antenna is obatiend for V-band applications.

3. Results and discussion

3.1. Antenna measurement setup

The simulation of the proposed antenna is carried out using finite element method based electromagnetic solver, High-frequency Structure Simulator (HFSS). To verify the proposed results, Lighted Programable Functional Keys (LPFK) machine is utilized to fabricate a sample prototype as depicted in Fig. 10. The Vector Network Analyzer (VNA) by Rhode & Schwarz (R&S ZVA110) is used to verify the reflection coefficient, as depicted in Fig. 10 (a). Far-field measurements are carried out in a shielded millimeter-wave anechoic chamber using commercial ORBIT/FR far-field measurement system. A detailed explanation of far-field measurements setup is also explained in [31].

3.2. Reflection coefficient

The comparison among predicted and measured results of the proposed wideband antenna for V-band applications is illustrated in Fig. 11. It is observed that the proposed antenna offers a simulated $|S_{11}| < -10$ dB impedance bandwidth of 16.1 GHz ranging from 56.1 to 72.2 GHz. On the other hand, the measured results show that the proposed antenna obtained a wide impedance bandwidth of 20.2 GHz ranging between 55.7 and 76.1 GHz, as depicted in Fig. 11. In general, a strong agreement between simulated and measured result is observed, however, the minor difference is due to one or more of the following reasons:

1. The connectors used for measurements are DC to 67 GHz (V) connectors which results in mismatching at higher frequency due to increased losses across the connectors.
2. The fabrication tolerance of the apparatus used for fabrication of the antenna.
3. The measurement setup tolerance due to usage of old wires.

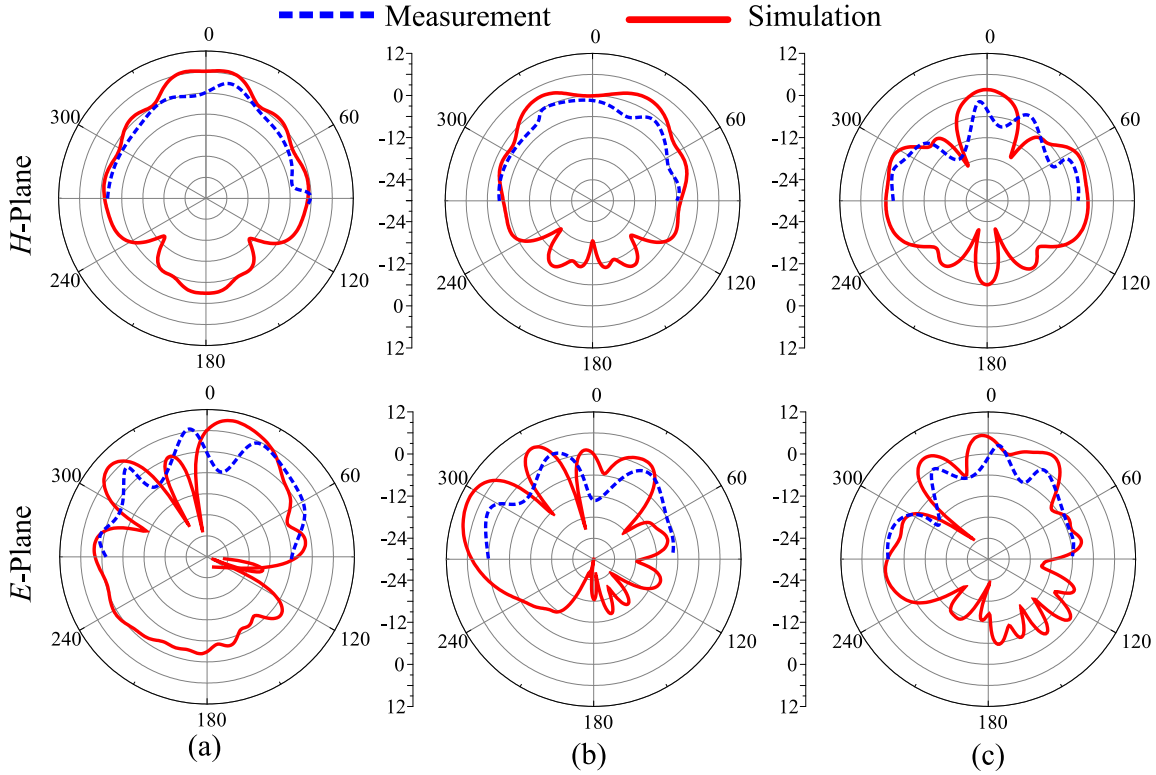

Fig. 12. The simulated and measured radiation patterns of the proposed antenna at selected frequencies of (a) 58 GHz, (b) 65 GHz, and (c) 70 GHz.

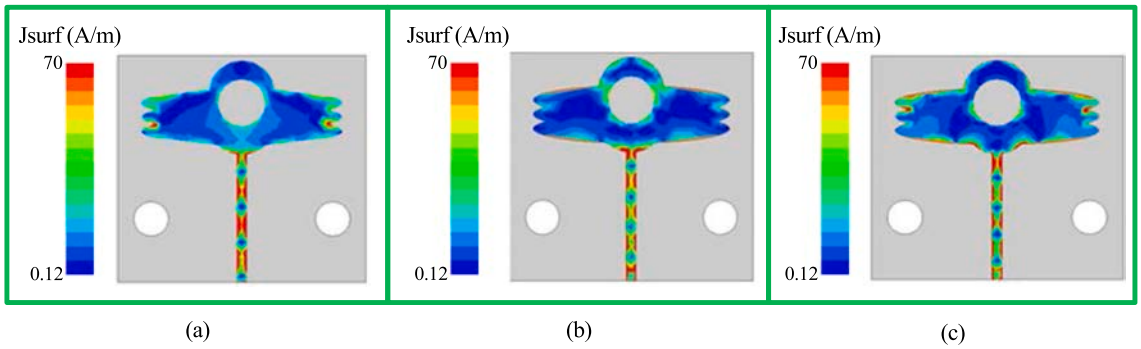

Fig. 13. The surface current distribution of the proposed antenna at (a) 58 GHz (b) 65 GHz (c) 70 GHz.

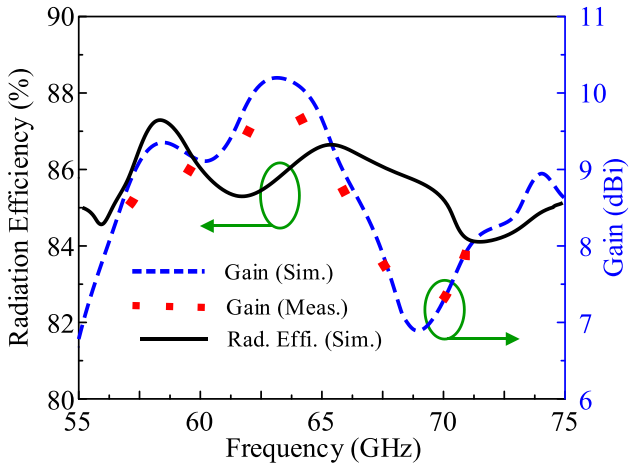

Fig. 14. Predicted peak gain and radiation efficiency of proposed V-band antenna.

3.3. Radiation pattern and surface current distribution

The radiation patterns of the proposed antenna at various frequencies are presented in Fig. 12 (a–c). Fig. 12 exhibits that antenna offers a broadside radiation pattern in principle *H*-plane ($\phi = 90^{\circ}$) where the main beam is pointed toward $\theta = 0^{\circ}$. While in principle *E*-plane ($\phi = 0^{\circ}$), a broadside radiation pattern is obtained for the selected frequencies of 58 GHz and 70 GHz, as demonstrated in Fig. 12 (a) and 12(c), respectively. Contrary to this, at 65 GHz it offers an end-fire like antenna where the main lobe is pointed towards -60^{0}, as shown in Fig. 12 (b).

To better understand the radiating mechanism of the proposed antenna, surface current distribution graphs are illustrated in Fig. 13. It is clearly exhibited that the maximum current is flowing through the feedline toward the radiator. Afterwards, for selected frequencies of 58 GHz and 70 GHz, the current distributes itself equally along the edges of elliptical stubs, as depicted in Fig. 13(a) and 13(c). On the other hand, Fig. 13 (b) shows that current density is also observed around the circular slot at 65 GHz, which causes the deviation in the radiation pattern.

3.4. Gain and efficiency

The measured and simulated results for gain and efficiency of the proposed antenna are presented in Fig. 14. The proposed antenna attained a gain of > 6.8 dBi over the entire operational band, whereas, the peak gain of 10.3 dBi is observed at 63.2 GHz, as illustrated in Fig. 14. Moreover, the antenna offers a radiation efficiency of > 84% throughout the operational band.

3.5. Comparison with state-of-the-art-work

Table 1 presents the comparative analysis of the proposed antenna

Table 1
Comparison of the proposed work with state-of-the-art-work for similar applications.

Ref. no.	Dimensions (mm × mm)	Dielectric Used	Relative Permittivity	Impedance Bandwidth (GHz)	Radiation Efficiency (%)	Peak Gain (dBi)	Design Technique
15	$1.9\lambda_0 \times 1.9\lambda_0$	Polyamide	2.8	57–64	–	–	Wearable button array antenna
16	$5.4\lambda_0 \times 5.4\lambda_0$	Rogers RO5880	2.2	54–66	78	11.8	Dual layer antenna
17	$2.85\lambda_0 \times 4.75\lambda_0$	Rogers RO3003	3	57–60.2	89.5	6.5	Microstrip patch antenna with dual patches used for dual frequencies band
18	$0.4\lambda_0 \times 0.4\lambda_0$	Benzo Cyclobutene (BCB)	2.65	55–65	77	0.8	Circularly polarized wire bond antenna
19	$3\lambda_0 \times 3.25\lambda_0$	Rogers RT5880	2.2	56–64	–	5–8	Antipodal vivaldi antenna
20	$0.75\lambda_0 \times 0.75\lambda_0$	Novel Material	3.8	45–65	87.5	–	Fractal T square antenna
21	$1.05\lambda_0 \times 1.94\lambda_0$	Ceramic substrate	9.9	61–64	76	10.7	Four element antenna array system by using gap couple technique
22	$3.3\lambda_0 \times 2.7\lambda_0$	Taconic TLY-5	2.2	57–66	–	28	Planner array antenna
23	$4.5\lambda_0 \times 5.75\lambda_0$	Taconic	2.2	52–67	–	10.63	Circularly polarized beam antenna array
24	$1.33\lambda_0 \times 2.65\lambda_0$	Taconic TaclamPlus	10.2	57–66	–	10	High permittivity substrate antenna
25	$2.28\lambda_0 \times 1.83\lambda_0$	Rogers RO4003	3.55	57.2–63.8	76.5	11.6	Monopole antenna array
26	$1.65\lambda_0 \times 2.15\lambda_0$	Liquid crystal polymer	2.9	49.91–52.15	88	6.18	Truncated ground plane printed dipole antenna
This work	$2.43\lambda_0 \times 2.24\lambda_0$	ROGERS RT5880	2.2	56.1–72.2	88	10.3	Patch antenna with fractal structure and slot

with recently reported literary works. It could be observed that most of the antennas offer wideband at the cost of large size, while the antennas with smaller size obtained low gain values. Moreover, it is observed from Table 1 that the structural complexity of the proposed antenna is low as the design technique adopted is simpler as compared to other antenna designs. Consequently, fabrication errors also decrease due to simple structure. Furthermore, usage of the full ground plane at the back of the antenna significantly reduces the backward radiation, thus making this antenna a potential candidate for both off-body and on-body applications. Hence, structural simplicity, ultra-wideband behavior, and high gain endorses the suitability of the proposed antenna for current and forthcoming communication systems.

4. Conclusions

A compact yet wideband and high gain antenna is presented in this paper. The geometrical structure of the antenna is inspired by a conventional circular patch antenna. The final proposed antenna is composed of a fractal circular patch with three elliptical stubs incorporated horizontally adjacent to each other. The presented antenna obtained an ultra-wide band with 16.1 GHz bandwidth ranging between 56.1 and 72.2 GHz. Furthermore, the antenna obtained a high peak gain value of 10.3 dBi over the frequency band. Also, antenna exhibits good radiation characteristics. Moreover, simulated and measured results demonstrate strong agreement. As the proposed antenna provides compact size, ultra-wide bandwidth, high gain, and good radiation efficiency, thus, it befits the V-band communication devices for both on-body and off-body applications.

Funding: This project has received funding from Universidad Carlos III de Madrid and the European Union's Horizon 2020 research and innovation program under the Marie Sklodowska-Curie Grant 801538. Also, this work is partially supported by the Researchers Supporting Project number (RSP-2021/58), King Saud University, Riyadh, Saudi Arabia.

Data Availability Statement: All research data have been included within manuscript.

Declaration: All research achievements including results, figures, tables, and etc are original and attained by the authors of this article and drawn by themselves.

Declaration of Competing Interest

The authors declare that they have no known competing financial interests or personal relationships that could have appeared to influence the work reported in this paper.

Acknowledgement

The authors sincerely appreciate the funding from Universidad Carlos III de Madrid and the European Union's Horizon 2020 research and innovation program under the Marie Sklodowska-Curie Grant 801538. Also, this work is partially supported by Antenna and Wireless Propagation Group (AWPG); https://sites.google.com/view/awpgrp, and from the Researchers Supporting Project number (RSP-2021/58), King Saud University, Riyadh, Saudi Arabia.

References

[1] Andrews JG, Buzzi S, Choi W, Hanly SV, Lozano A, Soong ACK, et al. What will 5G be? IEEE J Sel Areas Commun 2014;32(6):1065–82.
[2] Khajeh-Khalili F, Honarvar MA, Naser-Moghadasi M, Dolatshahi M. Gain enhancement and mutual coupling reduction of multiple-intput multiple-output antenna for millimeter-wave applications using two types of novel metamaterial structures. Int J RF Microwave Comput Aided Eng 2020;30(1). https://doi.org/10.1002/mmce:v30.110.1002/mmce:22006.
[3] Hussain M, et al. Simple Geometry Multi-Bands Antenna For Millimeter-Wave Applications At 28 GHz, 38 GHz, And 55 GHz Allocated To 5G Systems. In: 2021 46th International Conference on Infrared, Millimeter and Terahertz Waves (IRMMW-THz); 2021. p. 1–2. https://doi.org/10.1109/IRMMW-THz50926.2021.9567407.
[4] Khajeh-Khalili F, Honarvar MA, Naser-Moghadasi M, Dolatshahi M. High-gain, high-isolation, and wideband millimetre-wave closely spaced multiple-input multiple-output antenna with metamaterial wall and metamaterial superstrate for 5G applications. IET Microwaves Antennas Propag 2021;15(4):379–88.
[5] Hussain M, et al. Broad-Band Miniaturized Antenna Implementation Working Among 57–70 GHz V-Band for 5th Generation and Beyond Applications. In: 2021 46th International Conference on Infrared, Millimeter and Terahertz Waves (IRMMW-THz); 2021. p. 1–2. https://doi.org/10.1109/IRMMW-THz50926.2021.9567485.
[6] Siamarou AG, Al-Nuaimi M. A wideband frequency-domain channel-sounding system and delay-spread measurements at the license-free 57-to 64-GHz band. IEEE Trans Instrum Meas 2010;59(3):519–26.
[7] Rizvi SNR, Awan WA, Hussain N. Design and Characterization of Miniaturized Printed Antenna for UWB Communication Systems. J Electr Eng Technol 2020:1–8.
[8] Ghaffar A, Awan WA, Zaidi A, Hussain N, Rizvi SM, Li XJ. Compact Ultra Wide-Band and Tri-Band Antenna for Portable Device. Radioengineering 2020;29(4):601–8.
[9] Song CM, Trinh-Van S, Yi S-H, Bae J, Yang Y, Lee K-Y, et al. Analysis of Received Power in RF Wireless Power Transfer System With Array Antennas. IEEE Access 2021;9:76315–24. https://doi.org/10.1109/ACCESS.2021.3083270.
[10] Salamin MA, Ali WAE, Das S, Zugari A. Design and investigation of a multi-functional antenna with variable wideband/notched UWB behavior for WLAN/X-band/UWB and Kuband applications. AEU Int J Electron Commun 2019;111:152895. https://doi.org/10.1016/j.aeue.2019.152895.
[11] Hussain N, Awan WA, Naqvi SI, Ghaffar A, Zaidi A, Naqvi SA, et al. A Compact Flexible Frequency Reconfigurable Antenna for Heterogeneous Applications. IEEE Access 2020;8:173298–307.
[12] Hussain M, et al. A Wideband Antenna for V-Band Applications in 5G Communications. In: International Bhurban Conference on Applied Sciences and Technologies (IBCAST); 2021. p. 1017–9.
[13] Ali W, Das S, Medkour H, Soufian L. Planar dual-band 27/39 GHz millimeter-wave MIMO antenna for 5G applications. Microsyst. Technol. 2020;27:283–92.
[14] Hussain N, et al. Compact Wideband Patch Antenna and Its MIMO Configuration for 28 GHz Applications. AEU - International Journal of Electronics and Communications 2021;153612.
[15] Karthikeya GS, et al. Wearable button antenna array for V band application. In: In *2016 IEEE 5th Asia-Pacific Conference on Antennas and Propagation (APCAP)*; 2016. p. 283–4.
[16] Horst MJ, Ghasr MT, Zoughi R. Design of a compact V-band transceiver and antenna for millimeter-wave imaging systems. IEEE Trans Instrum Meas 2019;68(11):4400–11.
[17] Sharaf MH, Zaki AI, Hamad RK, Omar MMM. A novel dual-band (38/60 GHz) patch antenna for 5G mobile handsets. Sensors 2020;20(9):2541.
[18] Lin T-Y, Chiu T, Chang D-C. Design of V-Band Wide-Beamwidth Circularly Polarized Wire-Bond Antenna. IEEE Trans Compon Packag Manuf Technol 2018;8(2):261–8.
[19] Issa K, Fathallah H, Ashraf MA, Vettikalladi H, Alshebeili S. Broadband high-gain antenna for millimetre-wave 60-GHz band. Electronics 2019;8(11):1246. https://doi.org/10.3390/electronics8111246.
[20] Safia OA, Nedil M. Ultra-broadband V-band fractal T-square antenna. In: In *2017 IEEE International Symposium on Antennas and Propagation & USNC/URSI National Radio Science Meeting*; 2017. p. 2611–2.
[21] Hannachi C, Tatu SO. A Compact V-Band Planar Gap-Coupled 4×1 Antenna Array: Improved Design and Analysis. IEEE Access 2017;5:8763–70.
[22] Wu J, et al. A broadband high-gain planar array antenna for V-band wireless communication. In: In *Proceedings of 2014 3rd Asia-Pacific Conference on Antennas and Propagation*; 2014. p. 309–12.
[23] Park Y, Bang J, Choi J. Dual-circularly polarized 60 GHZ beam-steerable antenna array with 8× 8 butler matrix. Applied Sciences 2020;10(7):2413.
[24] Zelenchuk D, Fusco V, Goussetis G. V-band (57–66 GHz) planar antennas for WPAN applications. In: In *Proceedings of the 5th European Conference on Antennas and Propagation (EUCAP)*; 2011. p. 3122–5.
[25] Mneesy TS, Hamad RK, Zaki AI, Ali WAE. A Novel High Gain Monopole Antenna Array for 60 GHz Millimeter-Wave Communications. Applied Sciences 2020;10(13):4546.
[26] Usha Devi Y, Rukmini MSS, Madhav BTP. A compact conformal printed dipole antenna for 5G based vehicular communication applications. Progress in Electromagnetics Research C 2018;85:191–208.
[27] Naqvi AH, Park J, Baek C, Lim S. V-Band End-Fire Radiating Planar Micromachined Helical Antenna Using Through-Glass Silicon Via (TGSV) Technology. IEEE Access 2019;7:87907–15.
[28] Balanis CA. Antenna theory: analysis and design. John wiley & sons; 2016.
[29] Kumar M, Nath V. A high BDR microstrip-line fed antenna with multiple asymmetric elliptical wide-slots for wideband applications. Int J RF Microwave Comput Aided Eng 2020;30(7). https://doi.org/10.1002/mmce:v30.710.1002/mmce:22202.
[30] Kretzschmar JG. Wave propagation in hollow conducting elliptical waveguides. IEEE Trans Microw Theory Tech 1970;18(9):547–54.
[31] Naqvi AH, Park J, Baek C, Lim S. Via-Monopole Based Quasi Yagi-Uda Antenna for W-Band Applications using Through Glass Silicon via (TGSV) Technology. IEEE Access 2020;8:9513–9.

Musa Hussain received his bachelor's degree in electrical (Telecommunication) Engineering from COMSATS University Islamabad Campus in 2018. He secured his master's degree in electrical engineering from Bahria University Islamabad campus, Pakistan in 2020. His research interests include monopole patch antennas, 5G millimeter wave antennas, Frequency Reconfigurable antennas, Absorbers, Metamaterials and surfaces, and Frequency selective surfaces.

Syeda Iffat Naqvi received the B.Sc. Computer Engineering and the M.Sc. degree in Telecommunication Engineering from the University of Engineering and Technology Taxila, Pakistan, in 2006 and 2011, respectively. She secured her PhD degree in Telecommunication Engineering in 2021. She is currently serving as an Assistant Professor and also associated with the ACTSENA Research Group, University of Engineering and Technology Taxila. She has authored numerous scientific research articles in various prestigious international journals and conferences. Her professional services include but are not limited to Guest Editorship, Technical Program Committee member, University services, and reviewer for several international journals and conferences. Her research interests include 5G millimeter wave antennas, Reconfigurable antennas, Metamaterials, Beam steerable antennas, and smart antennas for 6G communication systems.

Wahaj Abbas Awan (S'20) received his BS. Degree in Electrical Engineering from the COMSATS University Islamabad, Sahiwal campus, Pakistan, in 2019. He was with Department of Integrated IT Engineering, Seoul National University of Science and Technology, Seoul, Republic of Korea from 2019 to 2021. He is currently pursuing the MS-Ph.D. Integrated Degree from Department of Information and Communication Engineering with the Chungbuk National University, Cheongju, Republic of Korea. He is also a working as a Research Assistant (RA) with the Optical Information Processing (OIP) laboratory under the supervision of Dr. Nam Kim. He authored more than 45 peer-reviewed conference and journal articles. He is also serving as reviewer for various journals which are not limited to International Journal of Microwave and Wireless Technologies, International Journal of Antenna and Propagation, Radio Engineering, MDPI-Applied Sciences, Intelligent Automation and Soft Computing (Autosoft Journal) and served as reviewer of various international conferences.

Wael Abd Ellatif Ali is currently Head of Quality Assurance Unit at College of Engineering and Technology (CET), Arab Academy for Science, Technology and Maritime Transport (AASTMT), Alexandria, Egypt. Furthermore, he is an Associate Professor in Electronics and Communications Engineering department, AASTMT, Alexandria, Egypt. He received his B.Sc. and MSc degrees in Electronics and Communication Engineering from AASTMT, Alexandria, Egypt, in 2004 and 2007, respectively. He holds the Ph.D. degree in Electrical Engineering from the Department of Electrical Engineering, University of Alexandria, Alexandria, Egypt, in 2012. His research interests include smart antennas, ⁋microstrip antennas, microwave filters, ⁋metamaterials, and MIMO antennas and its ⁋applications in wireless communications.

Esraa Mousa Ali is an assistant professor in Amman Arab University, where she is working in faculty of Aviation Sciences. She was born in Jordan in 1987, and received her B.E. degree in Electrical and computer engineering from Hashemite University in 2010. She received her M.S. degree in Electrical and Electronic Engineering from University Sains Malaysia (USM) in 2013. She received PhD degree at school of Electrical and Electronic Engineering, University Technology PETRONAS (UTP) in 2019. Her research area is about power electronics and microwave antenna.

Salahuddin Khan is an associate professor at king Saud University. He is specialized in design, modeling and simulation which can be extended to various fields of Electronics, Electromagnetic, and power Systems such as development of algorithms, realization of antenna devices, and power plant secondary systems. The above research lines have produced many research projects and publications. He has also contributed a US patent.

Mohammad Alibakhshikenari (Member, IEEE) was born in Mazandaran, Iran,in February 1988. He received the Ph.D. degree(Hons.) in electronic engineering from the University of Rome "Tor Vergata", Italy, in February 2020.He was a Ph.D. Visiting Researcher with the Chalmers University of Technology, Sweden, in 2018. His training during the Ph.D. included a research stage in the Swedish company Gap Waves AB. He is currently with the Department of Signal Theory and Communications, Universidad Carlos III de Madrid, Spain, as a Principal Investigator of the CONEX-Plus Talent Training Program and Marie Sklodowska-Curie Actions. His research interests include antennas and wave-propagations, metamaterials and metasurfaces, synthetic aperture radars (SAR), multiple-input multiple output (MIMO) systems, RFID tag antennas, substrate integrated waveguides (SIWs), impedance matching circuits, microwave components, millimeter-waves and terahertz integrated circuits, and electromagnetic systems. The above research lines have produced more than 130 publications on international journals, presentations within international conferences, and book chapters with a total number of the citations more than 2200 and H-index of 35. He was a recipient of the three years research grant funded by the Universidad Carlos III de Madrid and the European Union's Horizon 2020 Research and Innovation Program under the Marie Sklodowska-Curie Grant 801538 started in July 2021, the two years research grant funded by the University of Rome "Tor Vergata" started in November 2019, the three years Ph.D. Scholarship funded by the University of Rome "Tor Vergata" started in November 2016, and the two Young Engineer Awards of the 47th and 48th European Microwave Conference held in Nuremberg, Germany, in 2017, and in Madrid, Spain, in 2018, respectively. His research article entitled "High-Gain Metasurface in Polyimide On-Chip Antenna Based on CRLH-TL for Sub Terahertz Integrated Circuits" published in *Scientific Reports* was awarded as the Best Month Paper at the University of Bradford, in April 2020. He is serving as an Associate Editor for *IET Journal of Engineering* and *International Journal of Antennas and Propagation*. He also acts as a referee in several highly reputed journals and international conferences.